

INVITED

AB-INITIO EXCITED STATES CALCULATIONS FOR SEMICONDUCTOR MATERIALS: FROM BULK TO LOW DIMENSIONAL SYSTEMS

M. PALUMMO, M. BRUNO, R. DEL SOLE

*Dipartimento di Fisica Universita di Roma "Tor Vergata" Via della Ricerca Scientifica 1
00133 Roma, Italy*

S. OSSICINI

*INFN-S3 nanoStructures and bioSystems at Surfaces, Dipartimento di Scienze e Metodi dell'
Ingegneria, Universita di Modena e Reggio Emilia, Italy*

First-principles ground-state calculations on different kind of materials are currently carried out within density functional theory. On the other hand a correct description of the electronic excitations, which are at the origin of many experimental spectra, requires more refined theories. In this paper we summarize the main equations of the theoretical many-body approach used to describe electronic and optical properties of real materials. Some examples of excited state calculations in bulk and low dimensional semiconducting systems are given.

1 Introduction

Density functional theory (DFT) [1] is a single-particle approach that has achieved a great success to calculate ground state electronic properties of many-electron systems. However, when physical properties involving electronic excited states are required, this mean-field theory often fails in describing correctly experiments.

The use of many-body Green's functions theory [2], with DFT calculations as zero order approximation, is nowadays the state of the art to obtain quasi-particle excitation energies and dielectric responses in an increasing number of systems, from bulk materials, to surfaces and nanostructures. The theoretical framework is general and it will be described in the next section, while some examples of applications will be given in the last section.

2 Theoretical method

Here we will focus on the main equations of the density functional and many-body perturbation theories, referring the reader to reviews [3,4] for a complete description.

DFT is an approach to the study of the ground state properties of an N -electron system where the electron charge density $n(r)$, rather than the electron wave function, plays a central role. It has been introduced by Hohenberg and Kohn (HK)

in 1964 [1] when they showed how the ground state energy of a system of N interacting electrons in an external potential $V_{ext}(r)$ can be written as a functional of the ground state electronic density. In a later paper Kohn and Sham [1] reformulated the variational problem of minimizing the HK functional with respect to the charge density in terms of one-particle effective equations (Kohn-Sham equations), which are, nowadays, the most used strategy to perform DFT calculations. The self-consistent Kohn-Sham equations (KS) are the following [1]:

$$\left[-\frac{1}{2}\nabla^2 + V_{KS}^{eff}(\vec{r}) \right] \phi_i(\vec{r}) = \varepsilon_i \phi_i(\vec{r}), \quad (1)$$

with:

$$V_{KS}^{eff}(\vec{r}) = V_H(\vec{r}) + V_{xc}[n(\vec{r})] + V_{ext}(\vec{r}),$$

where $n(\vec{r}) = \sum_i f(\varepsilon_i) |\phi_i(\vec{r})|^2$ is the electron density, V_H is the Hartree potential, V_{xc} is the exchange-correlation potential defined as the functional derivative of the exchange-correlation part of the energy functional: $V_{xc} = \frac{\delta E_{xc}[n]}{\delta n}$. The most simple

and widely used approximation for $E_{xc}[n]$ is the so called local density approximation (LDA): $E_{xc}[n] = \int \varepsilon_{xc}[n] n(\vec{r}) d\vec{r}$ and $\varepsilon_{xc}[n]$ is the exchange-correlation energy per particle of an homogeneous electron gas of density $n(r)$ [5]. Several schemes beyond LDA have been introduced in the last decades, including a dependence on the density gradient as in generalized gradient approximation (GGA) giving, in some cases, a better description of the non locality of the exchange-correlation hole but without taking to systematic improvements in all kind of tested materials [6,7].

In any case, being the DFT a ground state theory, the KS eigenvalues cannot be interpreted as addition and removal electron energies, which instead can be formally obtained from an equation similar to the Kohn-Sham one, where a non hermitian, non local and energy-dependent operator, the self-energy appears, instead of the exchange-correlation potential [2]:

$$\left[-\frac{1}{2}\nabla^2 + V_{ext}(\vec{r}) + V_H(\vec{r}) \right] \Psi_i(\vec{r}, \omega) + \int d\vec{r}' \Sigma(\vec{r}, \vec{r}', \omega) \Psi_i(\vec{r}', \omega) = \varepsilon_i^{QP}(\omega) \Psi_i(\vec{r}, \omega).$$

This is the so-called "quasiparticle equation", which describes the extra hole created when an electron is extracted from the system (for example in a photoemission experiment or in an inverse photoemission experiment where the extra an electron is added to the system) and the polarization cloud that the other electrons create in order to screen it. A set of five integral equations, introduced by Hedin in 1965 [2], which relate the Green function G , the self-energy Σ , the irreducible polarization propagator P , the vertex Γ and the screened coulomb interaction W , allow in principle to obtain an expression for the self-energy. These equations are the following [2]:

$$G(12) = G_0(12) + \int d(34) G_0(13) \Sigma(34) G(42)$$

$$\Sigma(12) = i \int G(13) \Gamma(324) W(41) d(34)$$

$$P(12) = -i \int G(13) G(41) \Gamma(342) d(34)$$

$$\Gamma(123) = \delta(12)\delta(13) + \int \frac{\delta \Sigma(12)}{\delta G(45)} G(46) G(75) \Gamma(673) d(4567)$$

$$W(12) = v(12) + \int v(13) P(34) W(42) d(34)$$

(see [8] for the notation), where $v(1,2)$ is the bare Coulomb interaction and G_0 is the non-interacting Green-Function and the dielectric function is obtained as

$$\varepsilon(1,2) = \delta(1,2) - \int v(13) P(32) d(3).$$

Since the self-consistent solution of the Hedin equations is a very difficult task, both from theoretical and computational point of view [4,9], the standard practice, consolidated by the success of the applications, consists to stop at the first iteration step. In this way, starting with a diagonal form of the vertex function in time and space, a polarization function, given by non-interacting electron-hole pairs ($P = -iGG$, which is the random phase approximation, RPA) and a self-energy, product of the Green function G and the screened Coulomb interaction W , are obtained: this is the so-called GW method [2].

Moreover, the starting Green function is, generally, constructed using the single-particle Kohn-Sham orbitals and looking for a first-order perturbative solution of eq.2 with respect to $\Sigma - V_{xc}$. In this way the quasi-particle energies are obtained from the diagonal matrix elements of $\Sigma - V_{xc}$, as [4]:

$$\varepsilon_i^{QP} = \varepsilon_i^{LDA} + Z_i \langle \phi_i^{LDA} | \Sigma(\varepsilon_i^{LDA}) - V_{xc}^{LDA} | \phi_i^{LDA} \rangle,$$

with the renormalization constant $Z_i = 1 / (1 - \langle \phi_i^{LDA} | d\Sigma / d\varepsilon |_{\varepsilon=\varepsilon_i^{LDA}} | \phi_i^{LDA} \rangle)$.

The application of this approach yields, in many cases, energy levels in good agreement with photoemission and inverse photoemission experiments in semiconductors, insulators and metals [4,9].

On the other hand, in order to correctly describe spectroscopic processes, where electron-hole pairs are created [9], the inclusion of the self-energy corrections to the DFT eigenvalues in the RPA formula for P (which is the key quantity to obtain the measured spectra), is still not enough. In fact a two particle excited state must be described and this means that it is not possible to stop at the independent particle level in the description of P , but we have to introduce the electron-hole interaction (in other words a non delta-like Γ) through a second iteration of the Hedin equation [10]. This procedure allows to arrive to a four-index Dyson equation for P (see [10] for details of the derivation), which describes the electron-hole dynamics and reads as:

$$P(1234) = P_{IQP}(1234) + \int P_{IQP}(1256) K(5678) P(7834) d(5678),$$

and it is known as the Bethe-Salpeter equation (BSE).

Here P_{IQP} describes the polarizability of independent quasi-particle pairs of one hole and one electron while all the interactions are contained in the kernel K .

This kernel is done of two parts, which come by functional derivation, respectively, of the Hartree potential and of the self-energy, with respect to the single-particle Green function. Using the GW approximation for Σ and neglecting $\delta W/\delta G$ and dynamical effects in W , finally the kernel results as [10]:

$$K(1234) = \delta(12)\delta(34)v(13) - \delta(13)\delta(24)W(12).$$

It can be shown [10] that the first term, written in reciprocal space and eliminating the long-range divergent $G=0$ part, corresponds to the inclusion of local field effects (LF) (which arise when the system is non homogeneous on the microscopic scale), while the second represents the attractive screened electron-hole coulomb interaction (EXC). In the following examples we will see how the first term is particularly important in low dimensional systems, while the second one is, generally, the most important in bulk materials.

All the BSE calculations performed for insulators and semiconductors [10,11] show how the inclusion of the electron-hole Coulomb interaction allows a quantitative comparison with experiments, not only below the electronic gaps, where generally bound excitons are formed, but also above the continuum edge. One of the first examples appeared in the literature is given by bulk silicon [11] where excitonic effects have been shown to enhance the E_1 peak by almost 100%. Furthermore, the e-h interaction generally induces a redshift of the spectral peaks, which partially cancels the blueshift arising from the self-energy corrections.

3 Results and discussion

In the last ten years we assisted to a rapid growing up of application of this computational scheme to many materials from bulk semiconductors to real surfaces and nanostructures. Here we concentrate on a single material, germanium, showing the optical response of the bulk, of a surface and of some nanowires.

In Fig. 1 we compare the imaginary part of the bulk dielectric function obtained at different levels of the described theoretical approach, with the experimental curve [12]. This figure shows (although this example is not as explicative as bulk Si) how the agreement improves with the inclusion, beyond the self-energy corrections, of the local fields and excitonic effects.

To give more insight about the potentiality of the method we illustrate the case of a low dimensional system, where only their inclusion allows a quantitative agreement between the theoretical and experimental surface differential reflectivity spectra: the Ge(111)2x1 [13].

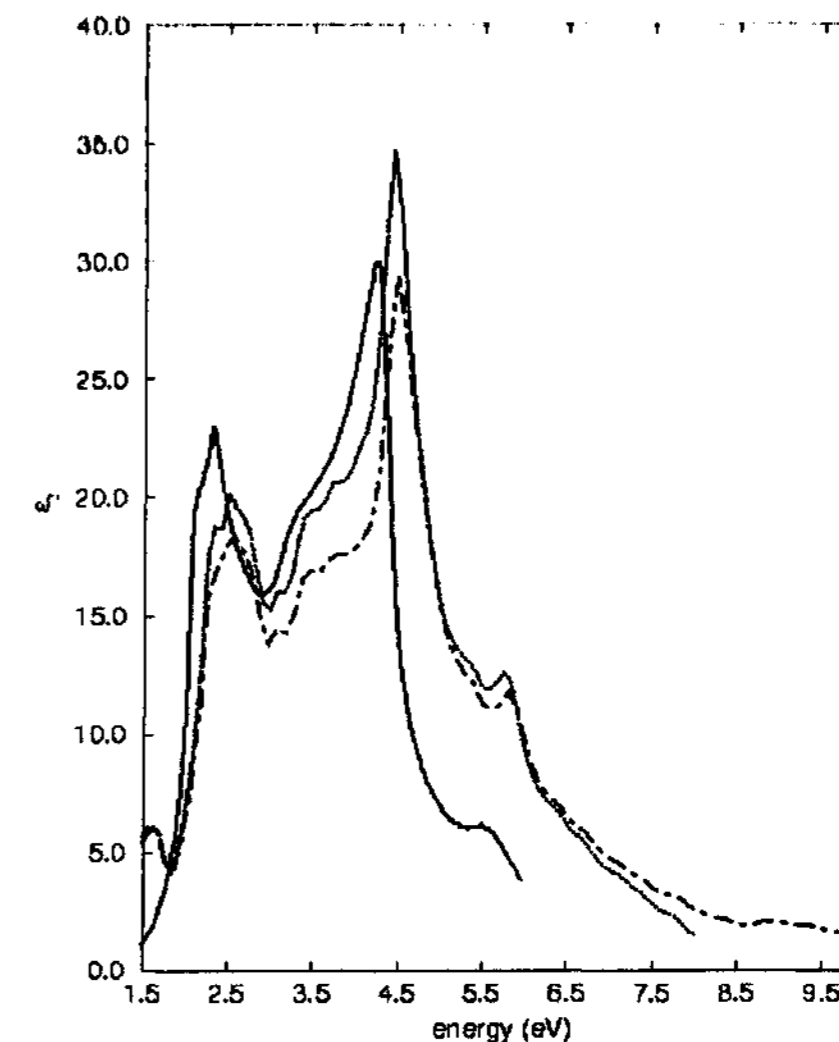


Figure 1. Imaginary part of the dielectric function of bulk Ge: experimental curve from [12] (solid line), the GW-RPA curve (dashed line), and with also the inclusion of excitonic and local-field effects (dotted line).

This is a particularly interesting surface, since it can exist in two different isomeric forms: one is the standard Pandey reconstruction, with buckled chains on the topmost layer; the other is an equivalent Pandey reconstruction, but where the chains undergo a ‘negative’ buckling (see Fig. 2). DFT-LDA ground-state calculations for the two isomers have shown them to be almost degenerate in energy. Hence, the uncertainties of the calculations (mainly due to the approximated form of the exchange-correlation potential), make it impossible, based only on total energy results, to predict the most stable form. Excited state calculations, instead, allow to make a clearer distinction between the positively and negatively buckled surfaces. In fact, the main surface peak in the reflectance difference spectra (RDS) is due to transitions involving essentially a single pair of flat surface bands, localized on the topmost layer. This peak appears to be redshifted by about 0.2 eV in the case of the negatively buckled chains, with respect to the standard Pandey geometry. For a useful comparison of the calculated spectra with the experiments *i.e.* to discriminate between the two isomers, it is necessary to know the absolute energy position of the theoretical peaks. This is possible if self-energy corrections, local-field and excitonic effects are taken into account explicitly. The results (Fig. 2(b)) strongly suggest the negatively buckled isomer as the dominant reconstruction of the measured sample. The existence of boundaries between positively and negatively buckled domains has also been revealed by STM experiments [14].

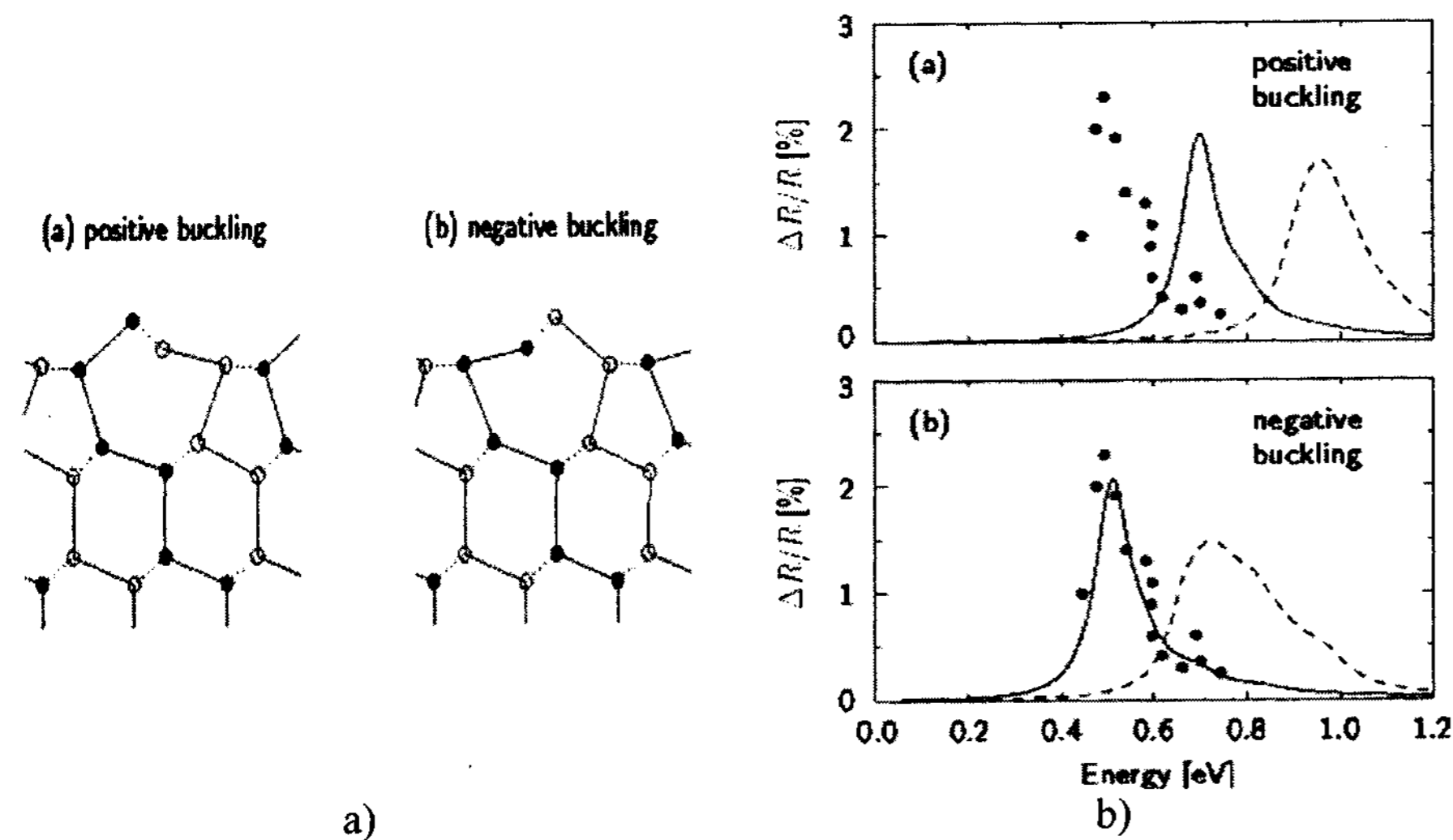


Figure 2. a: Side view of the two most isoenergetic structures of the Ge(111)2x1, displaying positive and negative buckling. b: Differential reflectivity spectrum of Ge(111)(2x1) surface: experimental data (dots) [15], theoretical curves [13]: dashed lines (GW), full lines (excitonic and local-field effects included).

As the last example we discuss some of the results obtained for freestanding hydrogen-terminated germanium wires oriented along [110] direction, with an effective width of 4 and 8 Å (an extended discussion about these wires, oriented also along the [100] and [111] directions, is presented elsewhere [16]). Starting with a study of the atomic relaxation effect on the wire band structures and dielectric responses, which we found to be very small, we obtained DFT-LDA bandstructures consistent with previous theoretical results obtained within a LAPW approach instead of a PP one (used to obtain all the results presented here) [17].

In Fig. 3 we plot some optical spectra calculated at the random phase approximation (RPA) (independent-particle) level with and without the inclusion of local-field (LF) effects. This shows how the dielectric response is strongly modified, in these confined 1-D systems, by taking into account their inhomogeneity (RPA+LF). In particular, including the local-field effects, we observe a small change of the optical spectrum for light polarized along the wire axis (x -direction, left panel), while we point out an important intensity reduction for the perpendicular light polarization (y -direction, right panel). The reason why the RPA, without LF, fails in the direction perpendicular to the wire axis is due to the depolarization effect which is created by the polarization charges induced in the system [18]. The depolarization is accounted for only if LFs are included, and is responsible of the suppression of the low energy absorption peaks in y direction, rendering the wire almost transparent below 8 eV.

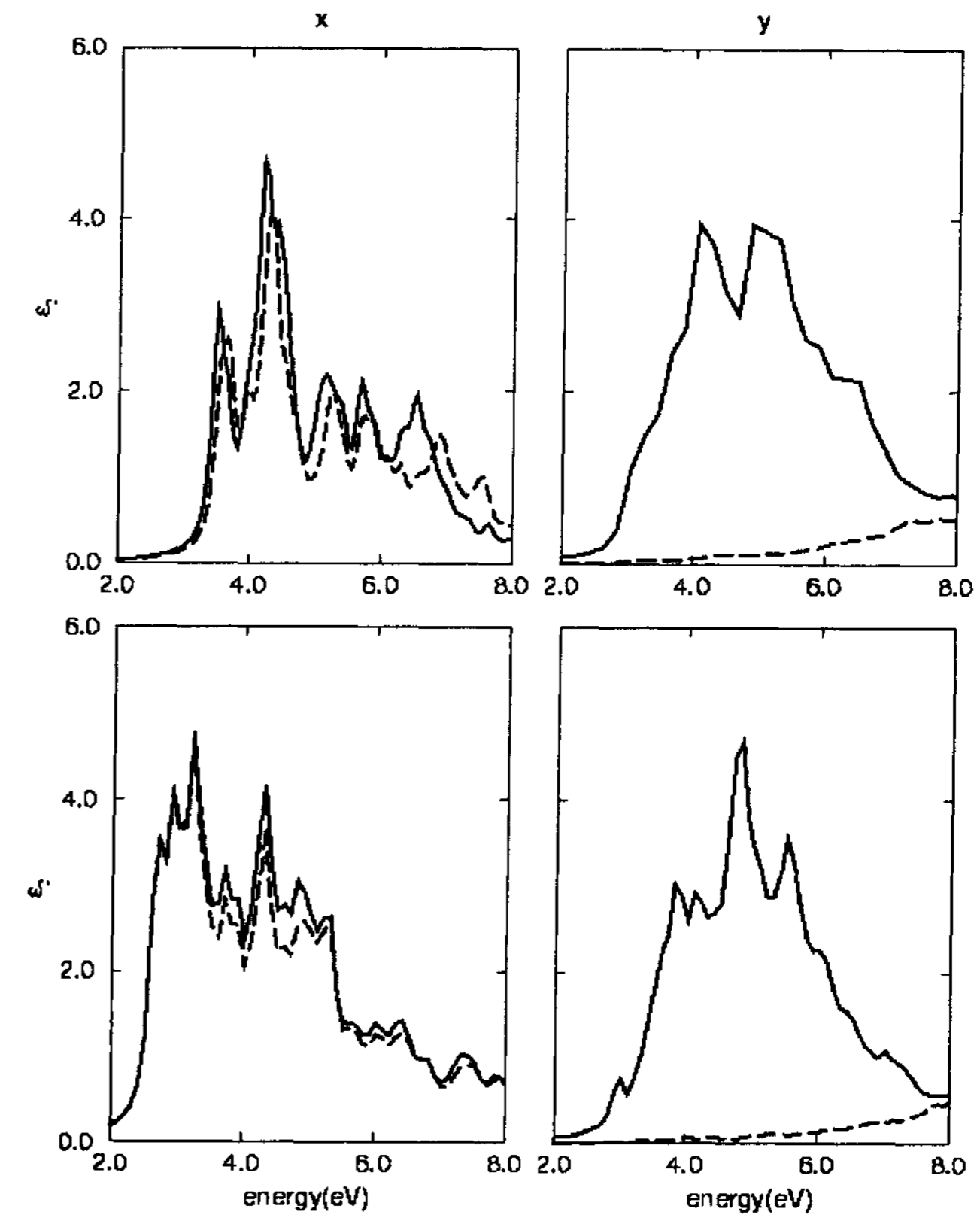


Figure 3. Theoretical imaginary part of the dielectric function polarized in the direction of the wire axis (left panel), and perpendicular to it (right panel) for (110) oriented Ge wires with different sizes: 4 Å (upper panels), 8 Å (lower panels). Solid lines: RPA, dashed lines: RPA+LF.

In ref. [16] other spectra, obtained overcoming the RPA but including both self-energy and e-h interaction show very important self-energy corrections, two or three times bigger than in bulk Ge as well as very strong e-h interactions, which sometimes seem, in some way, to balance at least in the energy peak positions.

Conclusion

The first-principles theoretical and computational scheme, obtained from a combination of density functional and many-body perturbation theories, which nowadays allow to obtain both ground and excited state properties of many materials, has been summarized here. Some examples, where many-body effects strongly influence the dielectric response have been also given.

Acknowledgements

This work has been supported by the INFM PAIS project "CELEX", MIUR COFIN-PRIN 2002 and by the EU's 6th Framework Programme through the NANOQUANTA NoE (NMP4-Ct-2004-500198). We acknowledge CINECA CPU time granted by INFM.

References

1. P. Hohenberg, W. Kohn, *Phys. Rev.* **136** B864 (1964); W. Kohn, L. J. Sham, *Phys. Rev.* **140** A1133 (1965).
2. L. Hedin, *Phys. Rev.* **139** A796 (1965).
3. R. M. Dreizler, E. K. U. Gross, *Density Functional Theory* (Springer, Heidelberg, 1990).
4. F. Aryasetiawan, O. Gunnarsson, *Rep. Prog. Phys.* **61** 237 (1998); W. G. J. Aulbur, J. W. Wilkins, *Solid State Physics*, ed. H. Ehrenreich, F. Spaepen (New York Academic, 1999) and references therein.
5. D. M. Ceperley, B. J. Alder, *Phys. Rev. Lett.* **45** 566 (1980).
6. J. P. Perdew, K. Burke, M. Ernzerhof, *Phys. Rev. Lett.* **77** 3865 (1996).
7. E. K. Gross, F. J. Dobson, M. Petersilka, *Density Functional Theory* (Springer, Heidelberg, 1996).
8. $\delta(r_1, t_1) \delta(r_1, t_2) = \delta(r_1 - r_2) \delta(t_1 - t_2)$.
9. W. Hanke, *Adv. Phys.* **27** 287 (1978).
10. G. Onida, L. Reining, A. Rubio, *Rev. Mod. Phys.* **5** 74 601 (2002) and references therein.
11. M. Rohlfing, S. G. Louie, *Phys. Rev. Lett.* **80** 3320 (1998); S. Albrecht, L. Reining, R. Del Sole, G. Onida, *Phys. Rev. Lett.* **80** 4510 (1998); L. X. Benedict, E. L. Shirley, R. B. Bohn, *Phys. Rev. Lett.* **80** 4514 (1998).
12. D. Aspnes, A. A. Studna, *Phys. Rev. B* **27** 985 (1983).
13. M. Rohlfing, M. Palummo, G. Onida, R. Del Sole, *Phys. Rev. Lett.* **85** 5440 (2000).
14. R. M. Feenstra, G. Meyer, F. Moresco, K. H. Rieder, *Phys. Rev. B* **64** 081306 (2001).
15. S. Nannarone, et al., *Solid State Comm.* **33** 593 (1980).
16. M. Bruno, et al., *submitted to Phys. Rev. Lett.*
17. A. N. Kholod, et al., *Phys. Rev. B* **70** 035317 (2004).
18. A. G. Marinopoulos, L. Reining, A. Rubio, N. Vast, *Phys. Rev. Lett.* **91** 046402 (2003).

INVITED

CONFINEMENT AND SYMMETRY EFFECTS IN ELECTRONIC AND OPTICAL PROPERTIES OF GERMANIUM NANOSTRUCTURES

A. N. KHOLOD^{1,2}, V. E. BORISENKO²

¹ Federal Office of Communications, P.O. Box, 2500 Biel, Switzerland

² Belarusian State University of Informatics and Radioelectronics

P. Browka 6, 220013 Minsk, Belarus

Germanium quantum size films and wires have been investigated regarding their electronic and optical properties. *Ab initio* calculations within the linearized augmented plane wave method have been employed for this purpose. Quantum confinement is found to shift the fundamental band gap of the bulk germanium to the blue energy range. The value of the upshift as well as the nature of the gap depends strongly on the surface symmetry. Strong direct gap absorption in the visible energy range has been predicted for germanium quantum films and wires.

1 Introduction

Scaling down of semiconductor structures to the nanometer length scale may modify radically material properties and related device concepts due to quantum mechanical effects [1]. In particular, quantum effects are considered to be a promising way of getting optoelectronic materials from indirect band-gap semiconductors. The idea is to use quantum confinement in order to transform the gap character from an indirect to a direct one, shift it up, and consequently provide light emission in the visible range. That is why the observation of strong visible luminescence of nanocrystalline silicon has stimulated great research interest in the physics of confined excitons in silicon (for a review see Ref. 2). The main expectation is that the luminescent silicon nanostructures may be used in integrated optoelectronic devices, which can be fabricated within the already well-established and highly advanced silicon technology [3].

Meanwhile, there is also an interest in other materials that in a nanocrystalline form could be used in optoelectronic components fabricated within silicon technology. Germanium (Ge) is considered to be a good candidate for that. Its combination with silicon (Si) has proved to possess a number of interesting properties [4]. It has been also shown theoretically that by varying the stress and geometry, one may get a direct band gap in Si/Ge superlattices [5-7].

However, the study of low-dimensional Ge structures has been mainly focused on quantum dots [8-12]. Other confined systems including quantum wires and quantum films made of this semiconductor should be mentioned as practically interesting objects. That stimulated our first *ab initio* quantum mechanical